# White Matter Microstructural Lateralization and Links to Language Function in Perinatal Stroke

**Bryce L. Geeraert**
University of Calgary
**Brian L. Brooks**
University of Calgary
**Adam Kirton**
University of Calgary
**Helen L. Carlson**
helen.carlson@albertahealthserivces.ca
University of Calgary

**Research Article**

**Keywords:** Perinatal stroke, language, white matter, neuroplasticity, NODDI

**Posted Date:** April 25th, 2024

**DOI:** https://doi.org/10.21203/rs.3.rs-4260180/v1



**Additional Declarations:** Competing interest reported. BLB receives royalties for the sales of the Pediatric Forensic Neuropsychology textbook (Oxford University Press), the Child and Adolescent Memory Profile (ChAMP, Sherman and Brooks, 2015, PAR Inc.), the Memory Validity Profile (MVP, Sherman and Brooks, 2015, PAR Inc.), and the Multidimensional Everyday Memory Ratings for Youth (MEMRY, Sherman and Brooks, 2017, PAR Inc.). BLB has a private practice where he evaluates youth who may have similar neurological histories. BLB also declares receiving honoraria for speaking engagements and external grants for research.

# Abstract

Perinatal strokes occur more commonly in the left hemisphere and often impact language areas, yet language disability only occurs in 20–25% of cases. Functional imaging studies investigating language processing have shown that perinatal stroke in the left hemisphere may result in contralesional shifts of activity, but none have investigated the structure of white matter connections in such altered language network conditions. Diffusion tensor imaging and neurite orientation dispersion and density imaging offer robust, microstructurally-sensitive metrics which can probe links between language-related tracts and function. In a sample of 73 participants with perinatal stroke and 32 typically-developing controls, we applied these methods to evaluate microstructure and lateralization of the arcuate fasciculus and uncinate fasciculus, two tracts classically associated with language. Furthermore, we examined associations between the microstructure of the contralesional arcuate and uncinate and language-based measures (i.e., verbal learning and verbal fluency) in children with unilateral perinatal stroke. We observed greater lateralization of white matter microstructure in the arcuate and uncinate for stroke participants than typically developing controls driven largely by differences in the ipsilesional hemisphere. Microstructure of the contralesional arcuate fasciculus was associated with both verbal learning and verbal fluency, while the contralesional uncinate fasciculus structure was associated with verbal fluency only. Overall, we demonstrate that white matter microstructure of bilateral language networks is impacted by unilateral perinatal stroke, and microstructural development of the arcuate and uncinate appear to be associated with language-based tests. Enhanced understanding of such functionally-relevant neuroplasticity may inform future rehabilitation strategies and intervention trials.


# INTRODUCTION

Perinatal stroke is a focal, vascular brain injury occurring between 20 weeks gestation and 28 days post birth (Raju et al., 2007). With an estimated prevalence of 1:1100 (Dunbar et al., 2020), perinatal stroke is a common disruptor of early neurological development. The two most common subtypes of perinatal stroke are arterial ischemic stroke (AIS), caused by cerebral artery occlusion, and periventricular venous infarction (PVI), caused by hemorrhage in the germinal matrix *in utero* (Dunbar & Kirton, 2018). In addition to frequently resulting in cerebral palsy and epilepsy, perinatal stroke can impact intelligence, executive function, and language (Kirton & deVeber, 2013; Lee et al., 2005; Murias et al., 2014). Cognitive performance following perinatal stroke varies broadly (Murias et al., 2014; Westmacott et al., 2010), and may be influenced by lesion size, location, and time of injury among other factors (Ballantyne et al., 2008; Westmacott et al., 2010). Children with combined cortical and subcortical lesions tend to exhibit the largest disruptions to cognitive function (Westmacott et al., 2010).

Perinatal stroke lesions are more common in the left hemisphere and most commonly caused by middle cerebral artery infarcts (AIS subtype), often directly impacting language areas (Ballantyne et al., 2008; Dunbar et al., 2020; Núñez et al., 2020; Stephan-Otto et al., 2017; Vargha-Khadem et al., 1991). However, the majority of children who experience perinatal stroke achieve near-normal language performance, with functional deficits observed in only 20–25% of cases (Anderson et al., 2011; Bates et al., 2001; Fuentes et

al., 2016; Kirton & deVeber, 2013; Lee et al., 2005; Murias et al., 2014; Stiles et al., 2005). This highlights the extraordinary ability of the brain to reorganize during early development; similar lesions during later childhood or adulthood can result in severe and permanent loss of language function. Remarkably, although language is typically left-lateralized, lesion side has only mild effects on outcomes (Ballantyne et al., 2007; Kirton & deVeber, 2013; Murias et al., 2014; Staudt, 2002). Language deficits may include more morphological errors, lower mean length of utterance, less complex syntax, and less detailed story settings (Avila et al., 2010; Demir et al., 2010; François et al., 2021; Reilly et al., 2013). Basic language skill is often preserved, with deficits observed when higher-level functions are tested (Ballantyne et al., 2007, 2008; Lee et al., 2005; Northam et al., 2018; Reilly et al., 2013; Westmacott et al., 2010). This suggests the developing brain can compensate for early damage to language areas, although the result may not be as efficient as a typical network.

Two reorganizational patterns may support language outcomes following a perinatal lesion (François et al., 2021; Murias et al., 2014). First, functional MRI studies of unilateral perinatal stroke have demonstrated a shift in processing to homologous language regions of the undamaged contralesional hemisphere (François et al., 2016, 2019; Guzzetta et al., 2008; Ilves et al., 2014; Jacola et al., 2006; Lidzba, 2007; Raja Beharelle et al., 2010; Staudt, 2002; Szaflarski et al., 2014; Tillema et al., 2008). Second, the language network may recruit remaining tissue in the ipsilesional hemisphere. Increased involvement of additional ipsilesional regions such as the posterior superior temporal gyrus or perilesional tissue has been associated with better language outcomes (Raja Beharelle et al., 2010; Vias & Dick, 2017). These two patterns are not mutually exclusive, and an altered interhemispheric balance in functional activity may be adaptive (Raja Beharelle et al., 2010).

While functional reorganization of language following perinatal stroke has been investigated, few studies have explored white matter connections underlying the language network (François et al., 2016, 2019; Heller et al., 2005; Northam et al., 2018). These studies assessed volumetric tissue damage and functional language outcomes and showed structural damage to left-hemisphere language tracts may result in a rightward shift of language function. However, as tissue volume is a non-specific metric, the conclusions drawn from these works should be considered preliminary. Studies employing metrics sensitive to white matter microstructure, such as diffusion-weighted MRI sequences, may provide new insight into neuroplasticity as related to language function, but no such studies exist to date.

Diffusion tensor imaging (DTI) is a popular diffusion-weighted MRI sequence that provides measurements of fractional anisotropy (FA), and mean, axial, and radial diffusivity (MD, AD, RD). These metrics are broadly sensitive to white matter microstructural features including myelin, axonal packing, axon permeability, and fiber coherence (Beaulieu, 2002). Beyond DTI, neurite orientation dispersion and density imaging (NODDI) provides the neurite density index (NDI) and orientation dispersion index (ODI) which are specific to axonal packing and fiber coherence, respectively (Zhang et al., 2012). Studies of brain development employing DTI and NODDI metrics have established that FA and NDI tend to increase while MD, AD, RD, and ODI tend to decrease with age. These trends suggest increases in axonal packing, myelin, and fiber coherence across healthy development (Chang et al., 2015; Geeraert et al., 2019; Mah et

al., 2017). DTI and NODDI metrics have also been applied in perinatal stroke to describe links between white matter and sensorimotor function (Craig et al., 2022; Hodge et al., 2017; Kuczynski et al., 2017, 2018; Mailleux et al., 2020; Nemanich et al., 2019).

Here, we applied DTI and NODDI to assess white matter microstructure of two primary language-related tracts, the arcuate fasciculus (AF) and uncinate fasciculus (UF), in children with unilateral perinatal stroke as compared to typically developing controls (TDC). We hypothesized that FA and NDI would be lower, while MD, AD, RD, and ODI would be higher in ipsilesional tissue, with the opposite trend observed in contralesional tissue. Furthermore, we hypothesized that perinatal stroke participants with higher FA and NDI and lower MD, AD, RD, and ODI in language-related tracts would perform better on tests of language function.

# METHODS

## Participants

Stroke participants were recruited via the Alberta Perinatal Stroke Project (APSP), a population-based research cohort (Cole et al., 2017). Inclusion criteria were: 1) unilateral perinatal stroke, confirmed by MRI using validated criteria (Kirton et al., 2008) including neonatal arterial ischemic stroke (NAIS), arterial presumed perinatal ischemic stroke (APPIS), or periventricular venous infarction (PVI) (Dunbar & Kirton, 2018), 2) age of 6 to 19 years and term birth (> 36 weeks), 3) symptomatic hemiparetic cerebral palsy (HCP), classified by a Pediatric Stroke Outcome Measure (PSOM) motor score > 0.5 (Kitchen et al., 2003), and perceived functional limitations by child and parent. Children with additional neurodevelopmental or psychiatric conditions, clinical or imaging evidence of bilateral stroke, diffuse injury, or unstable epilepsy were excluded. Children with NAIS and APPIS were combined into a single arterial ischemic stroke (AIS) group, due to similar mechanism of injury. Healthy control participants were recruited via a community-based healthy control recruitment program (www.hiccupkids.ca). Inclusion criteria for controls were: 1) 6 to 19 years of age and term birth (> 36 weeks), 2) absence of cognitive or motor deficits, and 3) right-handed. This study was conducted in accordance with the Declaration of Helsinki, and approved by the Conjoint Health Research Ethics Board at the University of Calgary (CHREB, ID: REB16-2535).

## Imaging

Participants completed an MRI scan using a 32-channel head coil on a GE 3T MR750w scanner (GE, Waukesha, WI). Diffusion-weighted images were acquired axially using spin-echo planar imaging (b = 750 s/mm$^2$, 32 non-collinear directions, 3 b = 0s/mm$^2$ volumes, 2.2mm isotropic voxel size, TR/TE = 11.5s/69ms, scan duration ~ 6:00). An additional diffusion-weighted sequence was acquired in a subset of participants (b = 2000 s/mm$^2$, 60 non-collinear directions, 5 b = 0 s/mm$^2$ volumes, 2.5mm isotropic voxel size, TR/TE = 15.0s/87ms, duration = ~ 16:00). High resolution T1-weighted images were obtained axially via a fast spoiled gradient echo brain volume (FSPGR BRAVO) sequence, with 1mm isotropic voxels (TR/TE = 8.6/3.2ms, flip angle = 11°, FOV = 256mm, scan duration = 5:00).

# Image Processing

Lesions were mapped by using MRIcro (Rorden & Brett, 2000) with the 3D painting tool on each subject's T1-weighted image. Initial selection was the darkest voxel within the lesion. Intensity difference and radius parameters were adjusted to expand the selection to the boundary between lesion and healthy tissue. Additional ROIs were added to cover the full lesion volume if needed. As voxels were 1mm isotropic, lesion size was equivalent to number of voxels included in the lesion. Due to the periventricular nature of PVI lesions, ipsilesional and contralesional ventricles were mapped, then lesion volume for PVI participants was calculated as contralesional ventricle volume subtracted from ipsilesional volume.

Diffusion-weighted data was processed using Tractoflow 2.1.1 (Theaud et al., 2019). Tractoflow offers a platform-independent pipeline for diffusion data processing, and includes artifact correction, anatomical registration, DTI metric calculation, fibre response function (FRF) and fibre orientation distribution function (fODF) calculation normalized to the cohort, and whole brain tractography. Diffusion datasets with b = 750 s/mm$^2$ were processed in Tractoflow for stroke and control cohorts separately. For participants where the b = 2000 s/mm$^2$ dataset was successfully collected, Tractoflow processing was repeated, then NDI and ODI maps were calculated using the NODDI toolbox (http://www.nitc.org/projects/noddi_toolbox) in Matlab R2019b (Mathworks, Natick, Mass., USA).

Following Tractoflow, the arcuate fasciculus (AF) and uncinate fasciculus (UF) were segmented via RecobundlesX, a semiautomated, reproducible method for tractography (Garyfallidis et al., 2018; Rheault, 2020). RecobundlesX performs well when reconstructing tracts which have been shifted, truncated, or made discontinuous, as is common in the lesioned hemisphere of perinatal stroke participants. Template tracts for RecobundlesX were generated using manually segmented tracts from five healthy control participants with high quality data and uninterrupted tracts. During manual segmentation of the AF, two regions of interest (ROIs) were placed using the color-coded FA map for reference. The first ROI was positioned on the coronal plane at the widest point of the anterior segment where the AF was primarily green (indicating anterior-posterior orientation), and the second ROI was placed on the axial plane where the projections into the temporal lobe were primarily blue (indicating superior-inferior orientation). For manual segmentation of the UF, two regions of interest were placed on the coronal plane at the widest point of anterior projections into the temporal pole and frontal lobe (Wakana et al., 2004). Additional ROIs were placed to remove spurious fibers where needed. Automated tract segmentation in RecobundlesX was performed 18 times per tract with small variations in tractography parameters. Streamlines that appeared in 50% or more trials were included in the final bundle. Tract segmentation was performed in both hemispheres and results were visually reviewed for accuracy. RecobundlesX outputs were transformed to binarized masks, and mean FA, MD, RD, AD, NDI, and ODI were calculated per tract.

Lateralization indices for each metric were calculated to assess balance between hemispheres using the following formula:

$$Lateralization = \frac{(contralesional - ipsilesional)}{(contralesional + ipsilesional)} * 100$$

such that larger negative lateralization indices indicated higher values in the ipsilesional hemisphere, while larger positive lateralization indices indicated higher values in the contralesional hemisphere. For our right-handed controls, the left hemisphere was treated as contralesional (dominant) and right as ipsilesional in the above equation, therefore positive indices indicated leftward lateralization. Positive lateralization values suggest more intact white matter microstructure in the contralesional hemisphere (or left, for controls) compared to the ipsilesional hemisphere for FA and NDI. *Negative* lateralization values reflect more intact white matter in the contralesional (or left) compared to ipsilesional hemisphere for MD, AD, RD, and ODI.

# Neuropsychological Assessments

A subset of perinatal stroke participants was previously referred for a clinical neuropsychological assessment battery if clinically indicated. Neuropsychological testing occurred during clinical assessments, thus age at language testing may have differed from age at MRI scan but both always occurred after the age of 6 years. Language-related tests included the California Verbal Learning Test – Children's Version (CVLT-C) and Word Generation-Initial Letter subtest from the Developmental Neuropsychological Assessment (NEPSY-II) (Korkman et al., 2007; Reilly et al., 2013). During the CVLT-C, participants were given five trials to learn as many words as they could from a list of 15 verbally presented nouns (List A). The CVLT-C List A Total Trials 1–5 T score was used as a metric of verbal learning. The Word Generation subtest of the NEPSY-II required participants to list as many words as they could (within a time limit) that begin with a specific letter (initial letter condition). The Semantic subtest required participants to generate as many words as they could within a certain semantic category (semantic condition). Word Generation – Initial Letter and Semantic scaled scores were employed here as a metric of verbal fluency. For both measures, higher values indicate better performance.

# Statistical Analyses

Statistical analyses were run in R v3.6.0 (R Core Team, 2020) and Jamovi (Love, J. et al., 2021). Normality of variables were tested using the Shapiro-Wilk test. For all analyses, the Benjamini-Hochberg false discovery rate (FDR) correction method was applied to correct for multiple comparisons (Benjamini & Hochberg, 1995).

Differences in age and sex distributions between TDC, AIS, and PVI cohorts were assessed using one-way ANOVA and chi-squared tests. Differences in lesion side prevalence between AIS and PVI cohorts was assessed via chi-squared test.

Group differences in imaging metrics for contralesional and ipsilesional hemispheres were assessed by one-way ANOVAs or ANCOVAs, controlling for age, sex, and lesion volume (stroke cohort only). Models that remained significant following FDR correction for 12 comparisons per hemisphere were followed up with post-hoc testing via TukeyHSD().

# Lateralization indices

One-sample t-tests were conducted via t.test in R to determine whether lateralization indices in each tract per group differed from a null distribution with mean of 0. Associations between lateralization indices and covariates of interest — controlling for covariates of no interest (as above) — were evaluated in each tract using linear regression via the linear model function *lm()* separately for each covariate. Covariates which were significant following FDR correction for three comparisons were included in follow-up analyses.

One-way ANOVAs—or ANCOVAs in the case of significant associations to one or more covariates—evaluated differences in lateralization indices for each metric in each tract, controlling for covariates as appropriate in each model. Post-hoc testing was conducted via TukeyHSD for significant ANOVAs. In the case of a significant association between lesion volume and lateralization, a follow-up ANCOVA was run for AIS and PVI participants controlling for lesion volume. ANOVAs evaluating differences in NDI and ODI were conducted between AIS and PVI participants only. Multiple comparisons were corrected using FDR for 12 tests.

# Language function

One-sample t-tests were run to evaluate whether CVLT-C T scores and Word Generation scaled scores differed from population norms of 50 and 10, respectively. Linear mixed models were run in a subset of perinatal stroke participants who had language assessments. Only DTI metrics were evaluated in these models, as NODDI imaging data was available for only six participants who underwent language testing. The following formula was used:

$$LanguageScore \sim DTImetric + Age + Sex + LesionVolume + Age * Sex$$

All variables were treated as fixed effects in these models. In the case that the age * sex interaction was not significant, it was removed and the model was re-run. FDR corrections for eight models were applied to account for multiple comparisons.

## RESULTS

# Participant Demographics and Clinical Language Measures

A total of 106 participants aged 6–19 years old were recruited, 73 of whom had perinatal stroke (38 AIS, 35 PVI). One participant with AIS was excluded from further analysis due to excessive head motion during their MRI resulting in poor image quality resulting in a total sample size of 105 participants (mean 12.3 ± 3.5 years, 45F / 60M). Demographic information and lesion characteristics for the final sample are summarized in Table 1. No differences were found for age ($F = 1.95$, $p = 0.15$) or sex distribution ($X^2 = 1.77$, $p = 0.41$) between TDC, AIS, and PVI groups. Lesion side prevalence was not different between AIS and PVI cohorts ($X^2 = 0.031$, $p = 0.86$).

Clinical language function scores are reported from the subset of perinatal stroke participants who were referred for assessment in Table 2. Word Generation – Initial Letter scaled scores were significantly lower than population norm ($t = -10.50$, $p < 0.001$), while CVLT-C List A Total Trials 1–5 T scores and Word Generation – Semantic condition scores did not differ from population norms (CVLT-C: $t = 0.23$, $p = 0.82$; Word Generation – Semantic: $t = -1.24$, $p = 0.23$). No group difference in language scores was observed between subjects with left versus right hemisphere lesions, although only 7 subjects with right hemisphere lesions had language scores available.

Table 1
Demographic information for typically developing controls (TDC) and participants with arterial ischemic stroke (AIS) and periventricular venous infarction (PVI) perinatal stroke.

| | TDC | AIS | PVI | Language Assessed |
|---|---|---|---|---|
| **Cohort size** | 32 | 38 | 35 | (see Table 2) |
| **Mean age at imaging (SD)** | 13.2 (3.54) | 12.1 (3.75) | 11.6 (3.10) | 13.42 (3.27) |
| **Mean age at NP assessment (SD)** | - | - | - | 10.83 (2.75) |
| **Sex** | 16 F / 16 M | 21 F / 17 M | 12 F / 23 M | 9 F / 15 M |
| **Stroke side** | | | | |
| **Left %** | - | 25 (65.8%) | 21 (60%) | 16 (66%) |
| **Median lesion volume, $cm^3$ (IQR)** | - | 43.9 (60.1) | 3.79 (11.3) | 35.3 (65.7) |

Table note: NP – neuropsychological, SD – standard deviation, IQR – interquartile range.

Table 2
Language assessment results for a subset of perinatal stroke participants.

| | Verbal Learning | Word Generation (Initial Letter) | Word Generation (Semantic) |
|---|---|---|---|
| **Sample Size** | 21 | 19 | 19 |
| **Age at test (SD)** | 10.6 (2.89) | 11.3 (2.52) | 11.3 (2.52) |
| **Sex** | 8F / 13M | 5F / 14M | 5F / 14M |
| **Stroke Type** | | | |
| **AIS** | 17 | 15 | 15 |
| **PVI** | 4 | 4 | 4 |
| **Stroke side (MRI)** | | | |
| **Left %** | 14 (66%) | 13 (68%) | 13 (68%) |
| **Median lesion volume, $cm^3$ (IQR)** | 47.4 (65.2) | 27.4 (61.4) | 27.4 (61.4) |
| **Mean score (SD)** | | | |
| **AIS** | 50.6 (12.8) | 4.67 (2.26) | 8.47 (3.70) |
| **PVI** | 50.3 (5.32) | 5.50 (1.73) | 10.5 (4.80) |
| **Overall** | 50.6 (11.6) | 4.84 (2.14) | 8.89 (3.90) |

Table note: The California Verbal Learning Test – Children's version (CVLT-C) was used to assess verbal learning. Scores reported are the CVLT-C trials 1–5 T score (CVLT-C Total 1–5). Word Generation subtests from the Developmental Neuropsychological Assessment – 2nd edition (NEPSY-II) were used to assess verbal fluency. Scaled scores are reported here. Each tests is positively scored such that higher numbers represent better performance. SD – standard deviation, IQR – interquartile range.

# Imaging

Lesion locations and sizes for the AIS and PVI subgroups are visualized in Fig. 1 where brighter areas represent more lesion overlap within each group.

RecobundlesX successfully segmented the arcuate and uncinate fasciculi in left and right hemispheres for all healthy controls. The ipsilesional arcuate fasciculus was successfully segmented in 6 AIS (15.8%) and 35 PVI (100%) participants, while the ipsilesional uncinate fasciculus was segmented in 26 AIS (68.4%) and 35 PVI (100%) participants. For contralesional tracts, the arcuate and uncinate fasciculi were segmented in 37 AIS (97%) and 35 PVI (100%) participants. Segmented tracts are shown in individual example participants for TDC, AIS, and PVI groups in Fig. 2. All imaging metrics were found to be normally distributed across our full sample and within each subgroup.

# Group Differences in Imaging Metrics per Hemisphere

Mean imaging metrics for all segmented tracts are summarized in Table 3 and Fig. 3. Group differences were found in the left or contralesional hemisphere uncinate fasciculus for FA ($F = 11.83$, $p < 0.001$), MD ($F = 5.08$, $p = 0.008$), and RD ($F = 9.19$, $p < 0.001$). Post-hoc testing revealed significantly lower FA for AIS and PVI groups compared to controls, higher MD for AIS compared to controls, and higher RD for AIS and PVI groups compared to controls.

In the right or ipsilesional hemispheres, significant differences were found in the arcuate fasciculus for FA ($F = 11.01$, $p < 0.001$), MD ($F = 14.98$, $p < 0.001$), AD($F = 10.38$, $p < 0.001$), and RD($F = 15.88$, $p < 0.001$), and in the uncinate fasciculus for FA ($F = 8.95$, $p < 0.001$), MD ($F = 6.17$, $p = 0.0031$), RD ($F = 8.84$, $p < 0.001$), and NDI ($F = -3.46$, $p = 0.001$). Post-hoc testing in the arcuate fasciculus revealed lower FA for AIS and PVI groups compared to controls, higher AD, MD, and RD for AIS participants compared to both PVI and TDC groups, and higher RD for PVI compared to TDC participants as well. Post-hoc testing in the uncinate fasciculus revealed lower FA for AIS participants compared to PVI and TDC groups, higher MD for AIS compared to PVI participants, and higher RD for AIS compared to both PVI and TDC groups. Finally, NDI was significantly higher for PVI compared to AIS participants in the ipsilesional hemisphere.

Table 3
Mean imaging metrics for the AF and UF by participant group.

| Group | Tract | Side | n | FA | MD | AD | RD | NDI | ODI |
|---|---|---|---|---|---|---|---|---|---|
| **TDC** | AF | L | 32 | 0.405 | 0.800 | 1.16 | 0.617 | - | - |
| | AF | R | 32 | 0.409 | 0.803 | 1.18 | 0.617 | - | - |
| | UF | L | 32 | 0.385 | 0.848 | 1.22 | 0.662 | - | - |
| | UF | R | 32 | 0.366 | 0.869 | 1.23 | 0.688 | - | - |
| **AIS** | AF | Contrales. | 37 | 0.388 | 0.814 | 1.17 | 0.636 | 0.498 | 0.327 |
| | AF | Ipsiles. | 6 | 0.368 | 0.924 | 1.29 | 0.742 | 0.443 | 0.311 |
| | UF | Contrales. | 37 | 0.357 | 0.869 | 1.22 | 0.694 | 0.444 | 0.327 |
| | UF | Ipsiles. | 26 | 0.342 | 0.884 | 1.22 | 0.717 | 0.417 | 0.349 |
| **PVI** | AF | Contrales. | 35 | 0.401 | 0.797 | 1.16 | 0.617 | 0.515 | 0.318 |
| | AF | Ipsiles. | 35 | 0.384 | 0.829 | 1.18 | 0.652 | 0.480 | 0.322 |
| | UF | Contrales. | 35 | 0.363 | 0.861 | 1.21 | 0.684 | 0.453 | 0.332 |
| | UF | Ipsiles. | 35 | 0.372 | 0.851 | 1.21 | 0.672 | 0.452 | 0.328 |

Table note: Tracts are presented as left and right for TDC, and in contralesional and ipsilesional hemispheres for AIS and PVI perinatal stroke participants. MD, AD and RD units reported are $*10^{-3}$

s/mm$^2$.

# Lateralization Indices and Group Differences

Lateralization indices are summarized below in Table 4. In the arcuate fasciculus, lesion volume was associated with lateralization of MD (t = -5.31, p < 0.001), AD (t = -4.69, p < 0.001), RD (t = -4.72, p < 0.001), and NDI (t = 2.47, p = 0.023), while age was associated with ODI lateralization (t = -2.27, p = 0.035). In the uncinate fasciculus, lesion volume was associated with lateralization of FA (t = 2.99, p = 0.0042), MD (t = -2.45, p = 0.017), RD (t -2.99, p = 0.004), NDI (t = 4.24, p < 0.001), and ODI (t = -2.24, p = 0.033). Sex was not associated with any imaging metric in either tract. As such, lesion volume and age (but not sex) were used as covariates in subsequent tests of lateralization differences for the metrics and regions above.

Table 4
Mean lateralization indices for the AF and UF in TDC, AIS, and PVI groups.

| Group | Tract | n | FA | MD | AD | RD | NDI | ODI |
|---|---|---|---|---|---|---|---|---|
| **TDC** | AF | 32 | -0.493 (2.14) | -0.242 (0.760) | -0.528* (1.20) | 0.0312 (1.09) | | |
| | UF | 32 | 2.54* (2.72) | -1.18* (0.824) | -0.320 (1.50) | -1.98* (1.06) | | |
| **AIS** | AF | 6 | 1.51 (7.18) | -6.02 (7.94) | -5.37 (9.26) | -6.51 (6.21) | 5.62 (2.11) | 3.49 (4.05) |
| | UF | 26 | 2.31 (5.79) | -0.807 (2.19) | 0.0467 (3.57) | -1.51 (1.65) | 2.68 (3.11) | -3.33 (5.59) |
| **PVI** | AF | 35 | 2.23* (3.89) | -1.93* (1.77) | -1.04* (2.46) | -2.75* (1.97) | 3.56* (1.97) | -0.550 (5.28) |
| | UF | 35 | -1.11 (4.26) | 0.561 (1.88) | 0.200 (2.91) | 0.891 (1.40) | 0.177 (1.07) | 0.880 (4.67) |

Note: Positive lateralization values indicate leftward (TDC) or contralesional (AIS, PVI) lateralization for FA and NDI. Negative lateralization values indicate leftward (TDC) or contralesional (AIS, PVI) lateralization for MD, AD, RD and ODI. Standard deviation is included in brackets. Lateralization indices that significantly differed from the null distribution are marked by *. AF - arcuate fasciculus, UF - uncinate fasciculus, FA - fractional anisotropy, MD, AD, RD - mean, axial, radial diffusivity, NDI - neurite density index, ODI - orientation dispersion index.

Lateralization indices did not significantly differ from the null distribution for any metrics in AIS participants. For PVI participants, lateralization indices significantly differed from the null distribution in the arcuate fasciculus for FA (t = 3.39, p = 0.00183), MD (t = -6.26, p < 0.001), AD (t = -2.96, p = 0.006), RD (t = -6.48, p < 0.001), and NDI (t = 7.68, p < 0.001), but for no metrics in the uncinate fasciculus. For TDC participants, lateralization indices significantly differed from the null distribution for AD in the arcuate fasciculus (t = -2.73, p = 0.0103), and for FA (t = 5.28, p < 0.001), MD (t = -8.12, p < 0.001), and RD (t = -7.45, p < 0.001) in the uncinate fasciculus.

One-way ANOVAs revealed significant group differences in lateralization of all metrics for both the arcuate and uncinate fasciculus, with the exception of RD in the uncinate fasciculus, as summarized in Table 5 and shown in Fig. 4. Significant differences between groups revealed by post-hoc tests are marked in Fig. 4, $p < 0.05$.

Table 5
Results from ANOVAs testing for group differences in laterality indices between groups.

| | | FA | MD | AD | RD | NDI | ODI |
|---|---|---|---|---|---|---|---|
| **Arcuate fasciculus** | F | 4.82 | 14.33 | 11.58 | 13.34 | 2.75 | 1.58† |
| | p | 0.011* | < 0.001* | < 0.001* | < 0.001* | 0.113 | 0.225 |
| | df | 2, 70 | 2, 70 | 2, 70 | 2, 70 | 1, 18 | 1, 18 |
| **Uncinate fasciculus** | F | 7.35 | 9.65 | 1.25 | 10.49 | 10.6 | 5.35 |
| | p | 0.001* | < 0.001* | 0.292 | < 0.001* | 0.003* | 0.028* |
| | df | 2, 90 | 2, 90 | 2, 90 | 2, 90 | 1, 30 | 1, 30 |

Table note: Group comparisons for NDI and ODI were between AIS and PVI only, all other comparisons were among TDC, AIS and PVI groups. † indicates an ANCOVA was run controlling for age. Significant findings after FDR corrections are marked by *. AF - arcuate fasciculus, UF - uncinate fasciculus, FA - fractional anisotropy, MD, AD, RD - mean, axial, radial diffusivity, NDI - neurite density index, ODI - orientation dispersion index.

Follow-up ANCOVAs were performed, controlling for lesion volume, to add context to lateralization differences observed between perinatal stroke subtype cohorts. Results from these ANCOVAs controlling for lesion volume are summarized in Table 6.

Table 6
Results from ANCOVAs testing for group differences in lateralization indices, controlling for lesion volume in AIS and PVI participants. Significant differences (after FDR corrections) are marked by *.

| | | FA | MD | AD | RD | NDI | ODI |
|---|---|---|---|---|---|---|---|
| **Arcuate fasciculus** | F | 1.23 | 0.995 | 11.90 | 0.0603 | 0.417 | 0.653 |
| | p | 0.274 | 0.325 | 0.001* | 0.807 | 0.526 | 0.430 |
| | df | 1, 37 | 1, 37 | 1, 37 | 1, 37 | 1, 18 | 1, 18 |
| **Uncinate fasciculus** | F | 1.47 | 2.25 | 0.389 | 2.23 | 1.58 | 1.45 |
| | p | 0.230 | 0.139 | 0.535 | 0.141 | 0.218 | 0.238 |
| | df | 1, 57 | 1, 57 | 1, 57 | 1, 57 | 1, 29 | 1, 29 |

# Links between Contralesional Imaging Metrics and Language Scores

Linear mixed models with significant imaging metric predictors of language measures are summarized in Table 7. CVLT-C scores were associated with contralesional FA and RD in the arcuate fasciculus, while Word Generation scores were associated with AD in the contralesional arcuate and RD in the uncinate fasciculus. Age, sex, and lesion volume were included but were not significantly related to language scores in any models. Figure 5 visualizes significant links between imaging metrics and language scores.

Table 7
Significant effects from linear mixed models showing links between contralesional hemisphere imaging metrics and language tests, controlling for age, sex, and lesion volume.

| **CVLT-C List A Total 1–5** | | | | | | |
|---|---|---|---|---|---|---|
| | Predictor | $R^2$ (adj) | df | β | t | p |
| **Arcuate** | FA | 0.12 | 16 | 0.56 | 2.29 | 0.036 |
| **Arcuate** | AD | 0.31 | 16 | 0.68 | 3.33 | 0.004* |
| **Word Generation – Initial Letter** | | | | | | |
| | Predictor | $R^2$ (adj) | df | β | t | p |
| **Arcuate** | FA | 0.19 | 14 | 0.54 | 2.23 | 0.043 |
| **Arcuate** | AD | 0.23 | 14 | -0.73 | -2.46 | 0.028 |
| **Word Generation – Semantic** | | | | | | |
| | Predictor | $R^2$ (adj) | df | β | t | p |
| **Arcuate** | FA | 0.20 | 14 | 0.57 | 2.36 | 0.033 |

Table note: Significant findings after FDR corrections are marked by *.

# DISCUSSION

# Lateralization of language tracts

Consistent with previous literature examining white matter microstructure (Banfi et al., 2019) and language task-fMRI (Brauer & Friederici, 2007; Holland et al., 2007; Sachs & Gaillard, 2003; Schlaggar et al., 2002; Szaflarski et al., 2006; Ulualp et al., 1998), TDC participants showed systematic structural lateralization to the left hemisphere in the uncinate (for three microstructural metrics), but weaker evidence for structural lateralization in the arcuate fasciculus (just one microstructural metric). Language-related hemispheric lateralization develops relatively late, possibly around age 10 (Schlaggar

et al., 2002), thus our sample (aged 6–19 years) has likely captured this important developmental phase. During typical development, FA and NDI values tend to increase, while diffusivity metrics (MD, AD, RD) and ODI tend to decrease. These trends reflect underlying changes in neurite density, axonal packing and, myelination (Geeraert et al., 2019; Lebel & Deoni, 2018). Thus, positive lateralization suggests more intact white matter in the contralesional hemisphere (or left, for controls) compared to the ipsilesional hemisphere for FA and NDI. *Negative* lateralization reflects more intact white matter in the contralesional hemisphere for diffusivity variables (MD, AD, RD), and ODI. Comparisons between lateralization patterns in typically developing controls and children with perinatal stroke could shed light on compensatory alterations in white matter after early injury.

In the largest sample to date investigating structural lateralization in perinatal stroke, we identified consistent differences in lateralization between perinatal stroke participants and controls. For AIS in the arcuate fasciculus, diffusivity metrics were lateralized towards the contralesional hemisphere. Follow-up analysis in each hemisphere separately indicated lateralization was driven by differences in ipsilesional microstructure, as diffusivity metrics were higher (and FA lower) in the ipsilesional hemisphere for AIS compared to controls while no group differences were observed in the contralesional hemisphere. This apparent lateralization to the contralesional hemisphere is consistent with language task-fMRI studies that have demonstrated a shift to homologous regions in the non-lesioned right hemisphere in children with left lesions (François et al., 2016, 2019; Guzzetta et al., 2008; Ilves et al., 2014; Jacola et al., 2006; Lidzba, 2007; Raja Beharelle et al., 2010; Staudt, 2002; Szaflarski et al., 2014; Tillema et al., 2008). The consistency of such a contralateral shift in multiple microstructural metrics in language-related white matter bundles provides converging evidence of possible contralateral compensatory mechanisms after early injury (Staudt, 2002).

In the uncinate fasciculus, no lateralization differences were observed between AIS and TDC groups. However, differences were seen for imaging metrics in both hemispheres (FA lower and RD higher) for AIS participants compared to controls. Lateralization assesses interhemispheric balance, thus microstructural alterations occurring in both hemispheres may not be reflected in lateralization indices. Interestingly, MD was higher in the contralesional uncinate compared to the left hemisphere of healthy controls, although no difference in lateralization was observed. Overall, our findings suggest significant disruption to the ipsilesional arcuate and uncinate fasciculus in AIS. The arcuate was most consistently affected, as AIS middle cerebral artery lesions are more likely to impact temporoparietal regions, as visualized in Figs. 1 and 2, than frontotemporal regions. This structural specificity for stroke-related damage may also have implications for language function based on stroke type.

For PVI participants, microstructure of both the arcuate and uncinate fasciculus differed from controls. However, direction of lateralization differences between PVI and controls was not consistent (see Fig. 4). In the arcuate fasciculus for the PVI group, lateralization indices suggested higher FA and lower diffusivity of contralesional white matter compared to controls. In the uncinate, the opposite trend was observed (lower FA and higher diffusivity). These observations were confirmed by underlying imaging metrics in individual hemispheres. Taken together, we can see that lateralization of the arcuate and

uncinate fasciculi are impacted differently by PVI lesions, with differences in arcuate lateralization driven by the ipsilesional hemisphere, while the opposite is true for the uncinate. Given that PVI-related damage is typically isolated to periventricular white matter, these differences are likely related to anatomical localization of lesions caused by differences in underlying stroke mechanisms.

Examining microstructural differences between perinatal stroke types may additionally shed light on differences in anatomical placement and underlying mechanisms of stroke. AIS and PVI groups showed differences in microstructural lateralization in both the arcuate and uncinate fasciculi. In the arcuate, diffusivity metrics were significantly higher for AIS compared to PVI participants in the ipsilesional hemisphere, and diffusivity lateralization indices showed significantly more lateralization to contralesional indices as a result. In the uncinate fasciculus, microstructural differences suggested more intact ipsilesional uncinate fasciculus for PVI participants. Additionally, NDI and ODI showed a contralesional shift in the uncinate of AIS participants, with near-zero lateralization values for metrics suggesting no corresponding shift in PVI participants. All differences in lateralization between AIS and PVI groups were driven by the ipsilesional hemisphere, further confirming the critical role that lesion location plays in reorganization of the language network. Differences in lesion mechanism (arterial versus venous) and therefore lesion location (MCA versus periventricular damage) also likely play a role in the differing patterns of lateralization between groups.

When lesion volume was factored out, many differences in white matter structure between AIS and PVI sub-groups were not retained. This suggests that perinatal stroke severity is an important indicator of white matter structural outcomes, at least for the regions investigated here. Further, RD, a putative marker of myelin, remains more contralesionally lateralized in the AIS group compared to PVI, suggesting some microstructural adaptations in the language network are unique to arterial ischemic perinatal stroke. Lateralization indices ranged from approximately 6 to -6 across our sample, which equates to interhemispheric differences of about 13%.

# Contralesional white matter and language function

Perinatal stroke participants scored lower than the population mean on the Word Generation task in the Initial Letter condition, but not for the Semantic condition. Furthermore, no differences in verbal memory were observed compared to the population mean. This suggests language deficits following perinatal stroke are domain-specific, rather than general, and likely vary by lesion size and location although more data is needed to verify this.

Lesion side did not seem to influence language outcomes, although this finding should be considered preliminary given the limited number of perinatal stroke subjects with right hemisphere lesions and language scores available (n = 7). Previous studies have also reported no effect of lesion side on language function in perinatal stroke, and proposed this is likely due to the early timing of injury, occurring very early in life before language has developed and lateralized (Ballantyne et al., 2007; Staudt, 2002).

More intact contralesional arcuate microstructure was linked to higher verbal memory and verbal fluency scores, as shown in Fig. 5. Specifically, FA of the arcuate fasciculus was associated with performance on all verbal memory and fluency tasks, while AD was associated with verbal memory, and fluency in the Initial Letter condition, but not Semantic. These findings are not consistent with the dorsal/ventral language processing model, which proposes a dorsal stream responsible for mapping sound to articulation, and a ventral stream responsible for mapping sounds to meaning (Catani et al., 2005; Saur et al., 2008). This model would suggest the arcuate would be related to word generation, while the uncinate fasciculus would be related to verbal memory. Our findings may show the language network in perinatal stroke undergoes neuroplastic reorganization, or may differ because this model is based on healthy, left-lateralized language networks, while we evaluated contralesional (typically right) hemisphere structure in perinatal stroke participants. Links to both verbal memory and fluency emphasize the importance of the arcuate fasciculus structure for language function. This coincides with functional work, which identified maturational status of the arcuate fasciculus as an important determinant of language processing accuracy and speed (Skeide et al., 2016).

Several other associations between white matter microstructure and verbal fluency were observed when lesion volume was excluded from models. FA and MD in the arcuate, and MD in the uncinate were associated with Word Generation – Initial Letter scores, while RD in the arcuate was associated with Word Generation – Semantic scores. This suggests additional nuance in neuroplastic compensation in response to stroke. Our findings also suggest lesion size plays an important role in determining language outcomes, in line with previous research (Westmacott et al., 2010).

# Limitations and future directions

The findings presented here must be considered in light of some limitations. First, this was a retrospective study design, and thus MRI imaging of patients with perinatal stroke occurred later than language testing, with a mean gap between tests and imaging of 2.6 years. Additionally, only those for whom cognitive assessment was deemed to be clinically warranted were referred for testing, thus no data was available for perinatal stroke participants with near-normal or severely impaired language abilities. Second, while tracts were successfully segmented in all typical controls, ipsilesional tracts were missing for many perinatal stroke participants, particularly for the AIS group where the ipsilesional AF was identified in only six participants. As such, we limited our analysis to the contralesional hemisphere where language tracts were reconstructed, but comparisons between lateralization indices or raw imaging metrics for AIS and other subgroups should be confirmed in a larger sample. Expansion to additional language-tracts, or adopting a network approach such as graph theory may reveal additional trends not identified here.

# CONCLUSIONS

We have shown consistent differences in lateralization of white matter microstructure in language-related tracts between perinatal stroke participants and healthy controls. Perinatal lesions often resulted in lateralization contralesional to the typical language network. However, in PVI participants, the ipsilesional uncinate fasciculus did not exhibit a contralesional shift. Microstructure of the contralesional arcuate

fasciculus was associated with verbal memory and verbal fluency, while the contralesional uncinate was associated with fluency only. In the largest study of perinatal stroke and language function to date, we have confirmed previous preliminary work suggesting that white matter in the language network changes following perinatal lesions, frequently resulting in a bias towards more intact tracts in the contralesional hemisphere, and the structure of these tracts is associated with language performance. Future work is needed to expand upon the trends shown here and investigate links between white matter microstructure throughout the brain and language performance in more detail.

# Declarations


## ACKNOWLEDGEMENTS

The authors wish to thank the participants and families who participated in this study, without whom this work would not have been possible.


## AUTHOR CONTRIBUTIONS

Author contributions included study conception and design (BLG, HLC, AK), data collection (BLB, HLC, AK), image processing and statistical analysis (BLG, HLC), interpretation of results (all authors), manuscript drafting (BLG, HLC), revisions (BLG, HLC, AK), and approval of the final version to be published (all authors).


### *Funding sources*

This project was supported by funding from the Canadian Institutes of Health Research (CIHR) and the University of Calgary BRAIN CREATE program, which is funded by the Natural Sciences and Engineering Research Council (NSERC).


### *Human ethics*

This study was conducted in accordance with the Declaration of Helsinki and approved by the Conjoint Health Research Ethics Board (CHREB) at the University of Calgary, ID: REB16-2535.

### *Consent to participate*

All participants provided written informed consent upon enrolment in this study.

### *Conflicts of interest*

BLB receives royalties for the sales of the Pediatric Forensic Neuropsychology textbook (Oxford University Press), the Child and Adolescent Memory Profile (ChAMP, Sherman and Brooks, 2015, PAR Inc.), the Memory Validity Profile (MVP, Sherman and Brooks, 2015, PAR Inc.), and the Multidimensional Everyday Memory Ratings for Youth (MEMRY, Sherman and Brooks, 2017, PAR Inc.). None of the assessment tests disclosed here were used in the current study. BLB has a private practice where he evaluates youth who

may have similar neurological histories. BLB also declares receiving honoraria for speaking engagements and external grants for research.

### *Availability of data and material*

Data used in this analysis is available upon request to the corresponding author.

# References


1. Anderson, V., Spencer-Smith, M., & Wood, A. (2011). Do children really recover better? Neurobehavioural plasticity after early brain insult. *Brain*, *134*(8), 2197–2221. https://doi.org/10.1093/brain/awr103
2. Avila, L., Riesgo, R., Pedroso, F., Goldani, M., Danesi, M., Ranzan, J., & Sleifer, P. (2010). Language and Focal Brain Lesion in Childhood. *Journal of Child Neurology*, *25*(7), 829–833. https://doi.org/10.1177/0883073809350724
3. Ballantyne, A. O., Spilkin, A. M., Hesselink, J., & Trauner, D. A. (2008). Plasticity in the developing brain: Intellectual, language and academic functions in children with ischaemic perinatal stroke. *Brain*, *131*(11), 2975–2985. https://doi.org/10.1093/brain/awn176
4. Ballantyne, A. O., Spilkin, A. M., & Trauner, D. A. (2007). Language Outcome After Perinatal Stroke: Does Side Matter? *Child Neuropsychology*, *13*(6), 494–509. https://doi.org/10.1080/09297040601114878
5. Banfi, C., Koschutnig, K., Moll, K., Schulte-Körne, G., Fink, A., & Landerl, K. (2019). White matter alterations and tract lateralization in children with dyslexia and isolated spelling deficits. *Human Brain Mapping*, *40*(3), 765–776. https://doi.org/10.1002/hbm.24410
6. Bates, E., Reilly, J., Wulfeck, B., Dronkers, N., Opie, M., Fenson, J., Kriz, S., Jeffries, R., Miller, L., & Herbst, K. (2001). Differential Effects of Unilateral Lesions on Language Production in Children and Adults. *Brain and Language*, *79*(2), 223–265. https://doi.org/10.1006/brln.2001.2482
7. Beaulieu, C. (2002). The basis of anisotropic water diffusion in the nervous system—A technical review. *NMR in Biomedicine*, *15*(7–8), 435–455. https://doi.org/10.1002/nbm.782
8. Benjamini, Y., & Hochberg, Y. (1995). Controlling the False Discovery Rate: A Practical and Powerful Approach to Multiple Testing. *Journal of the Royal Statistical Society: Series B (Methodological)*, *57*(1), 289–300. https://doi.org/10.1111/j.2517-6161.1995.tb02031.x
9. Brauer, J., & Friederici, A. D. (2007). Functional neural networks of semantic and syntactic processes in the developing brain. *Journal of Cognitive Neuroscience*, *19*(10), 1609–1623. https://doi.org/10.1162/jocn.2007.19.10.1609
10. Catani, M., Jones, D. K., & ffytche, D. H. (2005). Perisylvian language networks of the human brain. *Ann Neurol*, *57*(1), 8–16. https://doi.org/10.1002/ana.20319
11. Chang, Y. S., Owen, J. P., Pojman, N. J., Thieu, T., Bukshpun, P., Wakahiro, M. L. J., Berman, J. I., Roberts, T. P. L., Nagarajan, S. S., Sherr, E. H., & Mukherjee, P. (2015). White Matter Changes of Neurite

Density and Fiber Orientation Dispersion during Human Brain Maturation. *PLOS ONE*, *10*(6), e0123656. https://doi.org/10.1371/journal.pone.0123656

12. Cole, L., Dewey, D., Letourneau, N., Kaplan, B. J., Chaput, K., Gallagher, C., Hodge, J., Floer, A., & Kirton, A. (2017). Clinical Characteristics, Risk Factors, and Outcomes Associated With Neonatal Hemorrhagic Stroke: A Population-Based Case-Control Study. *JAMA Pediatrics*, *171*(3), 230. https://doi.org/10.1001/jamapediatrics.2016.4151
13. Craig, B. T., Kinney-Lang, E., Hilderley, A. J., Carlson, H. L., & Kirton, A. (2022). Structural connectivity of the sensorimotor network within the non-lesioned hemisphere of children with perinatal stroke. *Scientific Reports*, *12*(1), 3866. https://doi.org/10.1038/s41598-022-07863-4
14. Demir, Ö. E., Levine, S. C., & Goldin-Meadow, S. (2010). Narrative skill in children with early unilateral brain injury: A possible limit to functional plasticity: Narrative skill in children. *Developmental Science*, *13*(4), 636–647. https://doi.org/10.1111/j.1467-7687.2009.00920.x
15. Dunbar, M., & Kirton, A. (2018). Perinatal stroke: Mechanisms, management, and outcomes of early cerebrovascular brain injury. *The Lancet Child & Adolescent Health*, *2*(9), 666–676. https://doi.org/10.1016/S2352-4642(18)30173-1
16. Dunbar, M., Mineyko, A., Hill, M., Hodge, J., Floer, A., & Kirton, A. (2020). Population Based Birth Prevalence of Disease-Specific Perinatal Stroke. *Pediatrics*, *146*(5), e2020013201. https://doi.org/10.1542/peds.2020-013201
17. François, C., Garcia-Alix, A., Bosch, L., & Rodriguez-Fornells, A. (2021). Signatures of brain plasticity supporting language recovery after perinatal arterial ischemic stroke. *Brain and Language*, *212*, 104880. https://doi.org/10.1016/j.bandl.2020.104880
18. François, C., Ripollés, P., Bosch, L., Garcia-Alix, A., Muchart, J., Sierpowska, J., Fons, C., Solé, J., Rebollo, M., Gaitán, H., & Rodriguez-Fornells, A. (2016). Language learning and brain reorganization in a 3.5-year-old child with left perinatal stroke revealed using structural and functional connectivity. *Cortex*, *77*, 95–118. https://doi.org/10.1016/j.cortex.2016.01.010
19. François, C., Ripollés, P., Ferreri, L., Muchart, J., Sierpowska, J., Fons, C., Solé, J., Rebollo, M., Zatorre, R. J., Garcia-Alix, A., Bosch, L., & Rodriguez-Fornells, A. (2019). Right Structural and Functional Reorganization in Four-Year-Old Children with Perinatal Arterial Ischemic Stroke Predict Language Production. *Eneuro*, *6*(4), ENEURO.0447-18.2019. https://doi.org/10.1523/ENEURO.0447-18.2019
20. Fuentes, A., Deotto, A., Desrocher, M., deVeber, G., & Westmacott, R. (2016). Determinants of cognitive outcomes of perinatal and childhood stroke: A review. *Child Neuropsychology*, *22*(1), 1–38. https://doi.org/10.1080/09297049.2014.969694
21. Garyfallidis, E., Côté, M.-A., Rheault, F., Sidhu, J., Hau, J., Petit, L., Fortin, D., Cunanne, S., & Descoteaux, M. (2018). Recognition of white matter bundles using local and global streamline-based registration and clustering. *NeuroImage*, *170*, 283–295. https://doi.org/10.1016/j.neuroimage.2017.07.015
22. Geeraert, B. L., Lebel, R. M., & Lebel, C. (2019). A multiparametric analysis of white matter maturation during late childhood and adolescence. *Human Brain Mapping*, *40*(15), 4345–4356.

https://doi.org/10.1002/hbm.24706

23. Guzzetta, A., Pecini, C., Biagi, L., Tosetti, M., Brizzolara, D., Chilosi, A., Cipriani, P., Petacchi, E., & Cioni, G. (2008). Language Organisation in Left Perinatal Stroke. *Neuropediatrics*, *39*(03), 157–163. https://doi.org/10.1055/s-0028-1085465
24. Heller, S. L., Heier, L. A., Watts, R., Schwartz, T. H., Zelenko, N., Doyle, W., & Devinsky, O. (2005). Evidence of cerebral reorganization following perinatal stroke demonstrated with fMRI and DTI tractography. *Clinical Imaging*, *29*(4), 283–287. https://doi.org/10.1016/j.clinimag.2004.09.003
25. Hodge, J., Goodyear, B., Carlson, H., Wei, X.-C., & Kirton, A. (2017). Segmental diffusion properties of the corticospinal tract and motor outcome in hemiparetic children with perinatal stroke. *Journal of Child Neurology*, *32*(6), 550–559. https://doi.org/10.1177/0883073817696815
26. Holland, S. K., Vannest, J., Mecoli, M., Jacola, L. M., Tillema, J.-M., Karunanayaka, P. R., Schmithorst, V. J., Yuan, W., Plante, E., & Byars, A. W. (2007). Functional MRI of language lateralization during development in children. *International Journal of Audiology*, *46*(9), 533–551. https://doi.org/10.1080/14992020701448994
27. Ilves, P., Tomberg, T., Kepler, J., Laugesaar, R., Kaldoja, M.-L., Kepler, K., & Kolk, A. (2014). Different Plasticity Patterns of Language Function in Children With Perinatal and Childhood Stroke. *Journal of Child Neurology*, *29*(6), 756–764. https://doi.org/10.1177/0883073813489350
28. Jacola, L. M., Schapiro, M. B., Schmithorst, V. J., Byars, A. W., Strawsburg, R. H., Szaflarski, J. P., Plante, E., & Holland, S. K. (2006). Functional Magnetic Resonance Imaging Reveals Atypical Language Organization in Children Following Perinatal Left Middle Cerebral Artery Stroke. *Neuropediatrics*, *37*(1), 46–52. https://doi.org/10.1055/s-2006-923934
29. Kirton, A., Chen, R., Friefeld, S., Gunraj, C., Pontigon, A.-M., & deVeber, G. (2008). Contralesional repetitive transcranial magnetic stimulation for chronic hemiparesis in subcortical paediatric stroke: A randomised trial. *The Lancet Neurology*, *7*(6), 507–513. https://doi.org/10.1016/S1474-4422(08)70096-6
30. Kirton, A., & deVeber, G. (2013). Life After Perinatal Stroke. *Stroke*, *44*(11), 3265–3271. https://doi.org/10.1161/STROKEAHA.113.000739
31. Kitchen, L., Anderson, P., Friefeld, S., MacGregor, D., Curtis, R., Sofronas, M., Domi, T., & Deveber, G. (2003). A validation study of the pediatric stroke outcome measure. *Stroke*, *34*, 316–316.
32. Korkman, M., Kirk, U., & Kemp, S. (2007). *NEPSY II: Clinical and interpretive manual*. PsychCorp.
33. Kuczynski, A. M., Carlson, H. L., Lebel, C., Hodge, J. A., Dukelow, S. P., Semrau, J. A., & Kirton, A. (2017). Sensory tractography and robot-quantified proprioception in hemiparetic children with perinatal stroke: Sensory Tractography in Perinatal Stroke. *Human Brain Mapping*, *38*(5), 2424–2440. https://doi.org/10.1002/hbm.23530
34. Kuczynski, A. M., Dukelow, S. P., Hodge, J. A., Carlson, H. L., Lebel, C., Semrau, J. A., & Kirton, A. (2018). Corticospinal tract diffusion properties and robotic visually guided reaching in children with hemiparetic cerebral palsy. *Human Brain Mapping*, *39*(3), 1130–1144. https://doi.org/10.1002/hbm.23904

35. Lebel, C., & Deoni, S. (2018). The Development of Brain White Matter Microstructure. *NeuroImage*, *182*, 207–218. https://doi.org/10.1016/j.neuroimage.2017.12.097
36. Lee, J., Croen, L. A., Lindan, C., Nash, K. B., Yoshida, C. K., Ferriero, D. M., Barkovich, A. J., & Wu, Y. W. (2005). Predictors of outcome in perinatal arterial stroke: A population-based study. *Annals of Neurology*, *58*(2), 303–308. https://doi.org/10.1002/ana.20557
37. Lidzba, K. (2007). Development and lateralization of language in the presence of early brain lesions. *Developmental Medicine & Child Neurology*, *47*(11), 724–724. https://doi.org/10.1111/j.1469-8749.2005.tb01067.x
38. Love, J., Dropmann, D., Selker, R., Gallucci, M., Jentschke, S., & Balci, S. (2021). *The jamovi project* (1.6) [Computer software]. httpsL//www.jamovi.org
39. Mah, A., Geeraert, B., & Lebel, C. (2017). Detailing neuroanatomical development in late childhood and early adolescence using NODDI. *PLOS ONE*, *12*(8), e0182340. https://doi.org/10.1371/journal.pone.0182340
40. Mailleux, L., Franki, I., Emsell, L., Peedima, M.-L., Fehrenbach, A., Feys, H., & Ortibus, E. (2020). The relationship between neuroimaging and motor outcome in children with cerebral palsy: A systematic review—Part B diffusion imaging and tractography. *Research in Developmental Disabilities*, *97*, 103569. https://doi.org/10.1016/j.ridd.2019.103569
41. Murias, K., Brooks, B., Kirton, A., & Iaria, G. (2014). A Review of Cognitive Outcomes in Children Following Perinatal Stroke. *Developmental Neuropsychology*, *39*(2), 131–157. https://doi.org/10.1080/87565641.2013.870178
42. Nemanich, S. T., Mueller, B. A., & Gillick, B. T. (2019). Neurite orientation dispersion and density imaging quantifies corticospinal tract microstructural organization in children with unilateral cerebral palsy. *Human Brain Mapping*, *40*(17), 4888–4900. https://doi.org/10.1002/hbm.24744
43. Northam, G. B., Adler, S., Eschmann, K. C. J., Chong, W. K., Cowan, F. M., & Baldeweg, T. (2018). Developmental conduction aphasia after neonatal stroke: Conduction Aphasia. *Annals of Neurology*, *83*(4), 664–675. https://doi.org/10.1002/ana.25218
44. Núñez, C., Arca, G., Agut, T., Stephan-Otto, C., & García-Alix, A. (2020). Precise neonatal arterial ischemic stroke classification with a three-dimensional map of the arterial territories of the neonatal brain. *Pediatric Research*, *87*(7), 1231–1236. https://doi.org/10.1038/s41390-019-0724-x
45. R Core Team. (2020). *R: A language and environment for statistical computing* (3.6.0) [Computer software]. R Foundation for Statistical Computing. https://www.R-project.org/
46. Raja Beharelle, A., Dick, A. S., Josse, G., Solodkin, A., Huttenlocher, P. R., Levine, S. C., & Small, S. L. (2010). Left hemisphere regions are critical for language in the face of early left focal brain injury. *Brain*, *133*(6), 1707–1716. https://doi.org/10.1093/brain/awq104
47. Raju, T. N. K., Nelson, K. B., Ferriero, D., Lynch, J. K., & and the NICHD-NINDS Perinatal Stroke Workshop Participants. (2007). Ischemic Perinatal Stroke: Summary of a Workshop Sponsored by the National Institute of Child Health and Human Development and the National Institute of

Neurological Disorders and Stroke. *PEDIATRICS*, *120*(3), 609–616. https://doi.org/10.1542/peds.2007-0336

48. Reilly, J. S., Wasserman, S., & Appelbaum, M. (2013). Later language development in narratives in children with perinatal stroke. *Developmental Science*, *16*(1), 67–83. https://doi.org/10.1111/j.1467-7687.2012.01192.x
49. Rheault, F. (2020). Analyse et reconstruction de faisceaux de la matière blanche. *Computer Science. Université de Sherbrooke*.
50. Rorden, C., & Brett, M. (2000). Stereotaxic Display of Brain Lesions. *Behavioural Neurology*, *12*(4), 191–200. https://doi.org/10.1155/2000/421719
51. Sachs, B. C., & Gaillard, W. D. (2003). Organization of language networks in children: Functional magnetic resonance imaging studies. *Current Neurology and Neuroscience Reports*, *3*(2), 157–162.
52. Saur, D., Kreher, B. W., Schnell, S., Kümmerer, D., Kellmeyer, P., Vry, M.-S., Umarova, R., Musso, M., Glauche, V., Abel, S., Huber, W., Rijntjes, M., Hennig, J., & Weiller, C. (2008). Ventral and dorsal pathways for language. *Proceedings of the National Academy of Sciences*, *105*(46), 18035–18040. https://doi.org/10.1073/pnas.0805234105
53. Schlaggar, B. L., Brown, T. T., Lugar, H. M., Visscher, K. M., Miezin, F. M., & Petersen, S. E. (2002). Functional neuroanatomical differences between adults and school-age children in the processing of single words. *Science (New York, N.Y.)*, *296*(5572), 1476–1479. https://doi.org/10.1126/science.1069464
54. Skeide, M. A., Brauer, J., & Friederici, A. D. (2016). Brain Functional and Structural Predictors of Language Performance. *Cerebral Cortex*, *26*(5), 2127–2139. https://doi.org/10.1093/cercor/bhv042
55. Staudt, M. (2002). Right-Hemispheric Organization of Language Following Early Left-Sided Brain Lesions: Functional MRI Topography. *NeuroImage*, *16*(4), 954–967. https://doi.org/10.1006/nimg.2002.1108
56. Stephan-Otto, C., Núñez, C., Arca, G., Agut, T., & García-Alix, A. (2017). Three-Dimensional Map of Neonatal Arterial Ischemic Stroke Distribution From Early Multimodal Brain Imaging. *Stroke*, *48*(2), 482–485. https://doi.org/10.1161/STROKEAHA.116.014186
57. Stiles, J., Reilly, J., Paul, B., & Moses, P. (2005). Cognitive development following early brain injury: Evidence for neural adaptation. *Trends in Cognitive Sciences*, *9*(3), 136–143. https://doi.org/10.1016/j.tics.2005.01.002
58. Szaflarski, J. P., Allendorfer, J. B., Byars, A. W., Vannest, J., Dietz, A., Hernando, K. A., & Holland, S. K. (2014). Age at stroke determines post-stroke language lateralization. *Restorative Neurology and Neuroscience*, *32*(6), 733–742. https://doi.org/10.3233/RNN-140402
59. Szaflarski, J. P., Holland, S. K., Schmithorst, V. J., & Byars, A. W. (2006). fMRI study of language lateralization in children and adults. *Human Brain Mapping*, *27*(3), 202–212. https://doi.org/10.1002/hbm.20177
60. Theaud, G., Houde, J.-C., Boré, A., Rheault, F., Morency, F., & Descoteaux, M. (2019). *TractoFlow: A robust, efficient and reproducible diffusion MRI pipeline leveraging Nextflow & Singularity* [Preprint].

Neuroscience. https://doi.org/10.1101/631952

61. Tillema, J.-M., Byars, A. W., Jacola, L. M., Schapiro, M. B., Schmithorst, V. J., Szaflarski, J. P., & Holland, S. K. (2008). *Reprint of "Cortical reorganization of language functioning following perinatal left MCA stroke" [Brain and Language 105 (2008) 99–111] q*. 11.
62. Ulualp, S. O., Biswal, B. B., Yetkin, F. Z., & Kidder, T. M. (1998). Functional magnetic resonance imaging of auditory cortex in children. *The Laryngoscope*, *108*(12), 1782–1786.
63. Vargha-Khadem, F., Isaacs, E. B., Papaleloudi, H., Polkey, C. E., & Wilson, J. (1991). DEVELOPMENT OF LANGUAGE IN SIX HEMISPHERECTOMIZED PATIENTS. *Brain*, *114*(1), 473–495. https://doi.org/10.1093/brain/114.1.473
64. Vias, C., & Dick, A. S. (2017). Cerebellar Contributions to Language in Typical and Atypical Development: A Review. *Developmental Neuropsychology*, *42*(6), 404–421. https://doi.org/10.1080/87565641.2017.1334783
65. Wakana, S., Jiang, H., Nagae-Poetscher, L. M., van Zijl, P. C. M., & Mori, S. (2004). Fiber Tract–based Atlas of Human White Matter Anatomy. *Radiology*, *230*(1), 77–87. https://doi.org/10.1148/radiol.2301021640
66. Westmacott, R., Askalan, R., Macgregor, D., Anderson, P., & Deveber, G. (2010). Cognitive outcome following unilateral arterial ischaemic stroke in childhood: Effects of age at stroke and lesion location. *Developmental Medicine & Child Neurology*, *52*(4), 386–393. https://doi.org/10.1111/j.1469-8749.2009.03403.x
67. Zhang, H., Schneider, T., Wheeler-Kingshott, C. A., & Alexander, D. C. (2012). NODDI: Practical in vivo neurite orientation dispersion and density imaging of the human brain. *NeuroImage*, *61*(4), 1000–1016. https://doi.org/10.1016/j.neuroimage.2012.03.072

# Figures

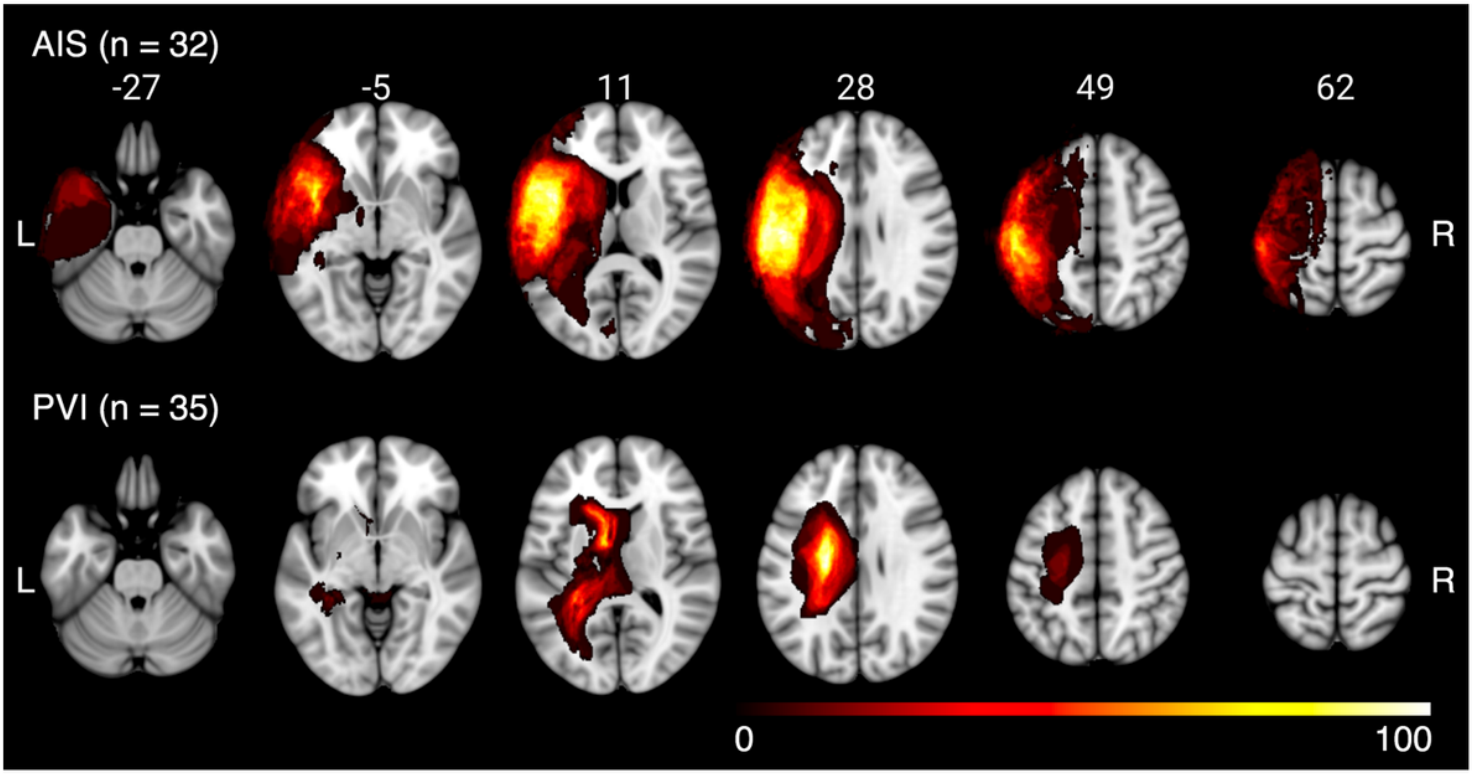


Figure 1

Lesion locations for participants with arterial ischemic stroke (AIS) or periventricular venous infarction (PVI). Lesion locations are presented as heatmaps, colored by percentage of participants with lesioned tissue in an area. For this visualization, lesion maps were registered to MNI space, and images from patients with right hemisphere lesions were reoriented to show the contralesional hemisphere on the left for all participants.

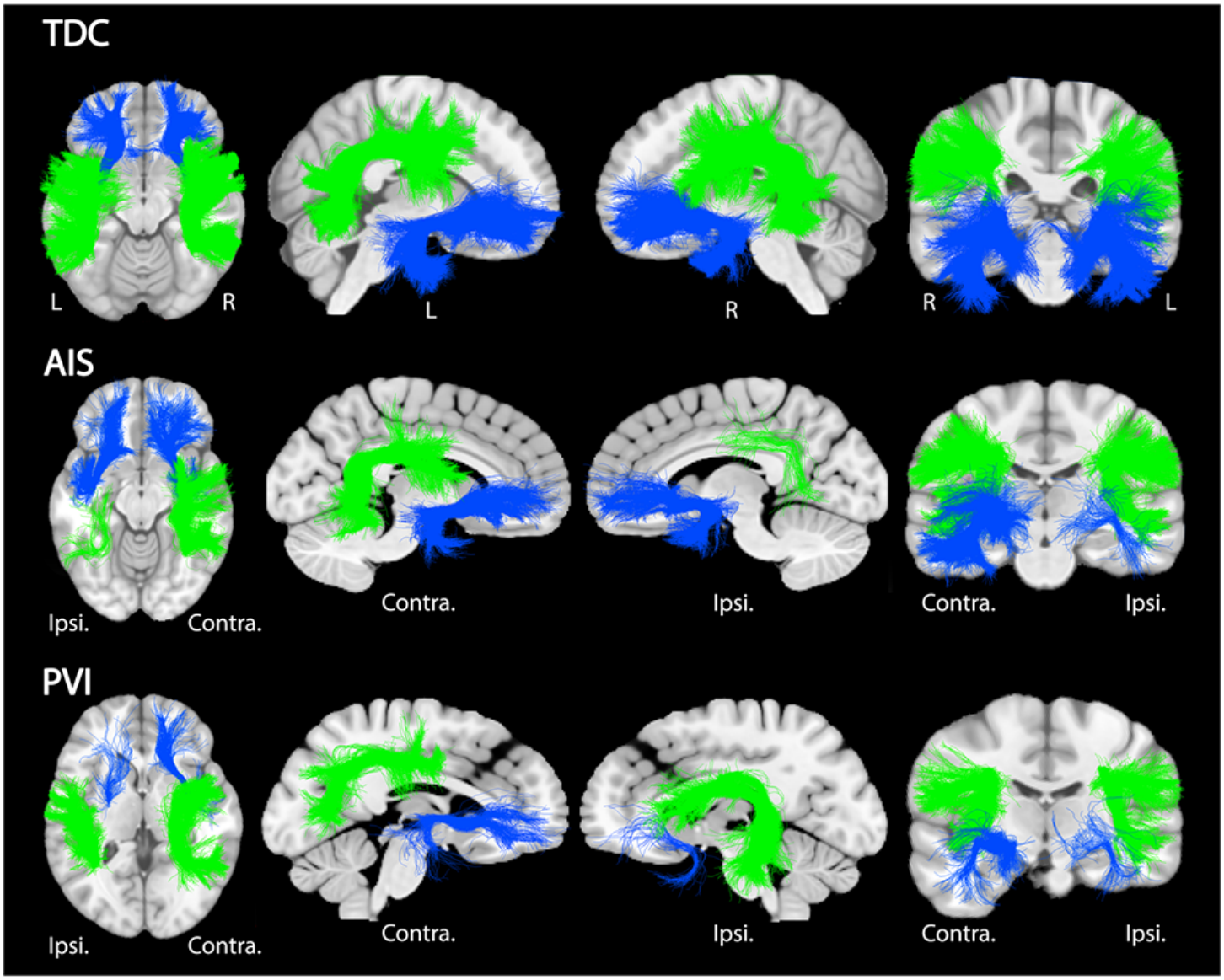


Figure 2

Sample tract masks for the arcuate fasciculus (green) and uncinate fasciculus (blue) from exemplar participants in TDC, AIS, and PVI cohorts overlaid on the MNI 152 template. Tracts were segmented via RecobundlesX, with five manually segmented tracts from the TDC group provided for reference. Ipsi – ipsilateral to the stroke lesion, Contra – contralateral to the lesion.

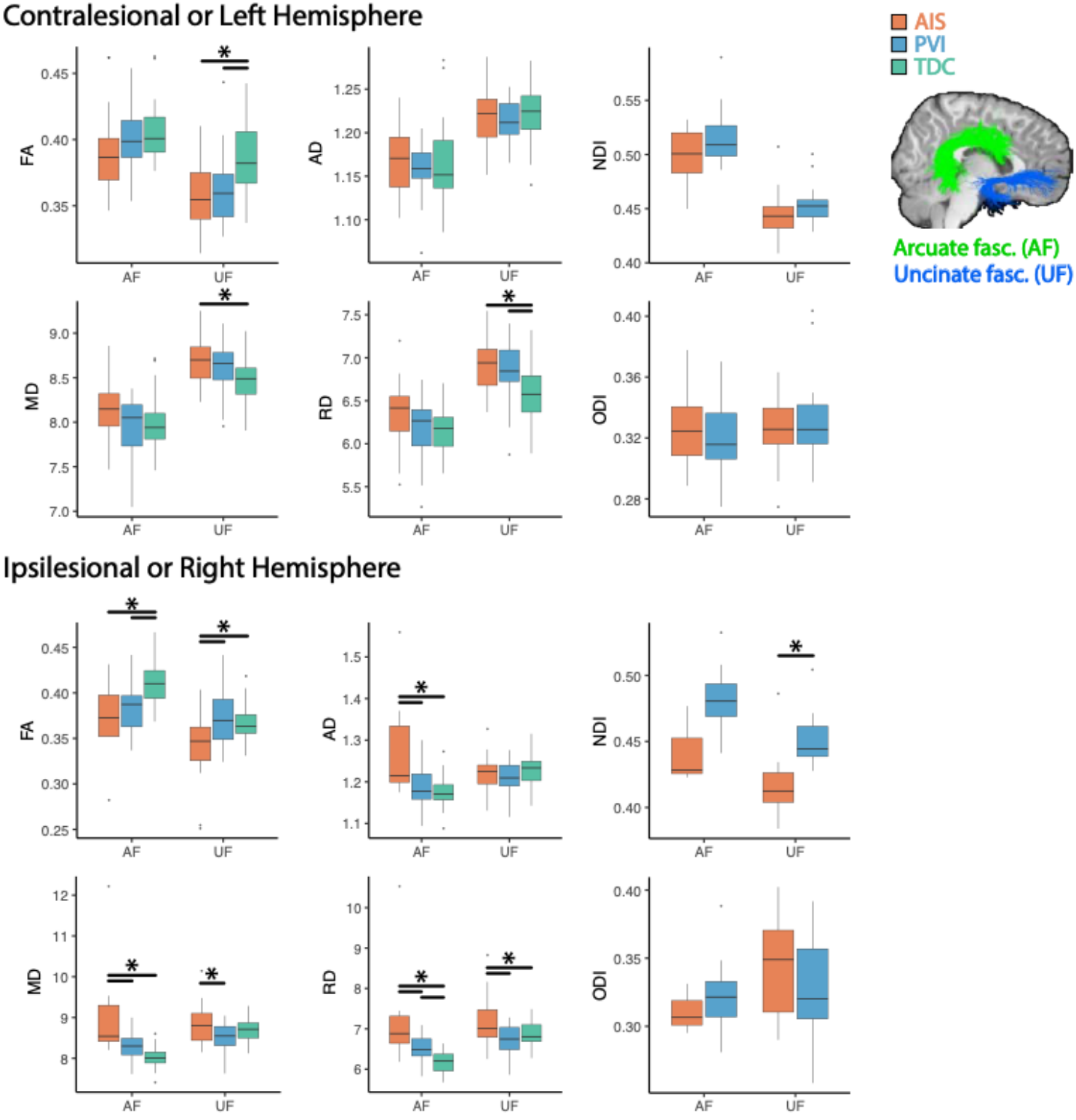


Figure 3

Mean imaging metrics for AIS and PVI perinatal stroke participants, and typically developing controls. For controls, the left hemisphere was treated as equivalent to the contralesional hemisphere, while right hemisphere was treated as ipsilesional. Significant differences between groups (after FDR corrections) are marked by *. AD units: $10^{-3}$ s/mm$^2$, MD and RD units: $10^{-4}$ s/mm$^2$.

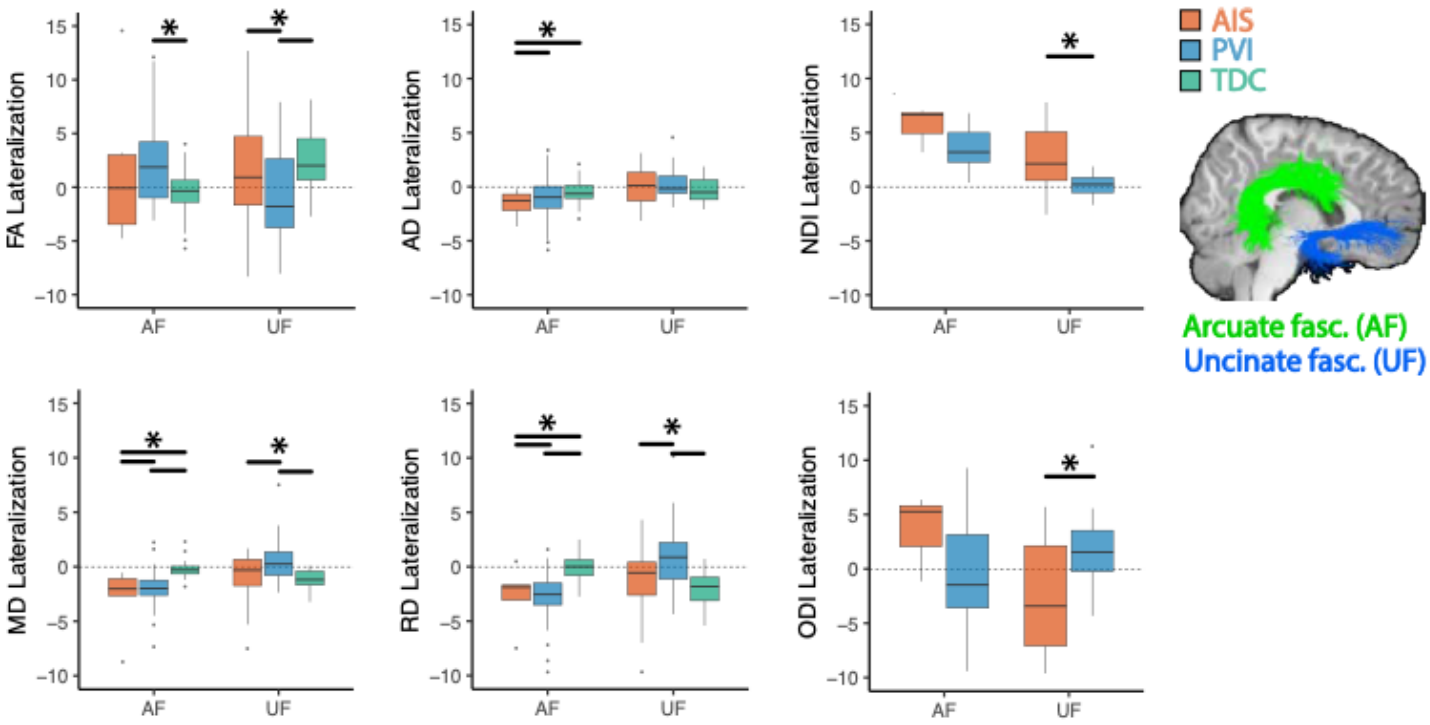


Figure 4

Differences in lateralization of imaging metrics between AIS and PVI perinatal stroke participants and typically developing controls (TDC). Positive values indicate higher metric values in the contralesional hemisphere, or the left hemisphere in controls. Significant differences between groups (after FDR corrections) are marked by *.

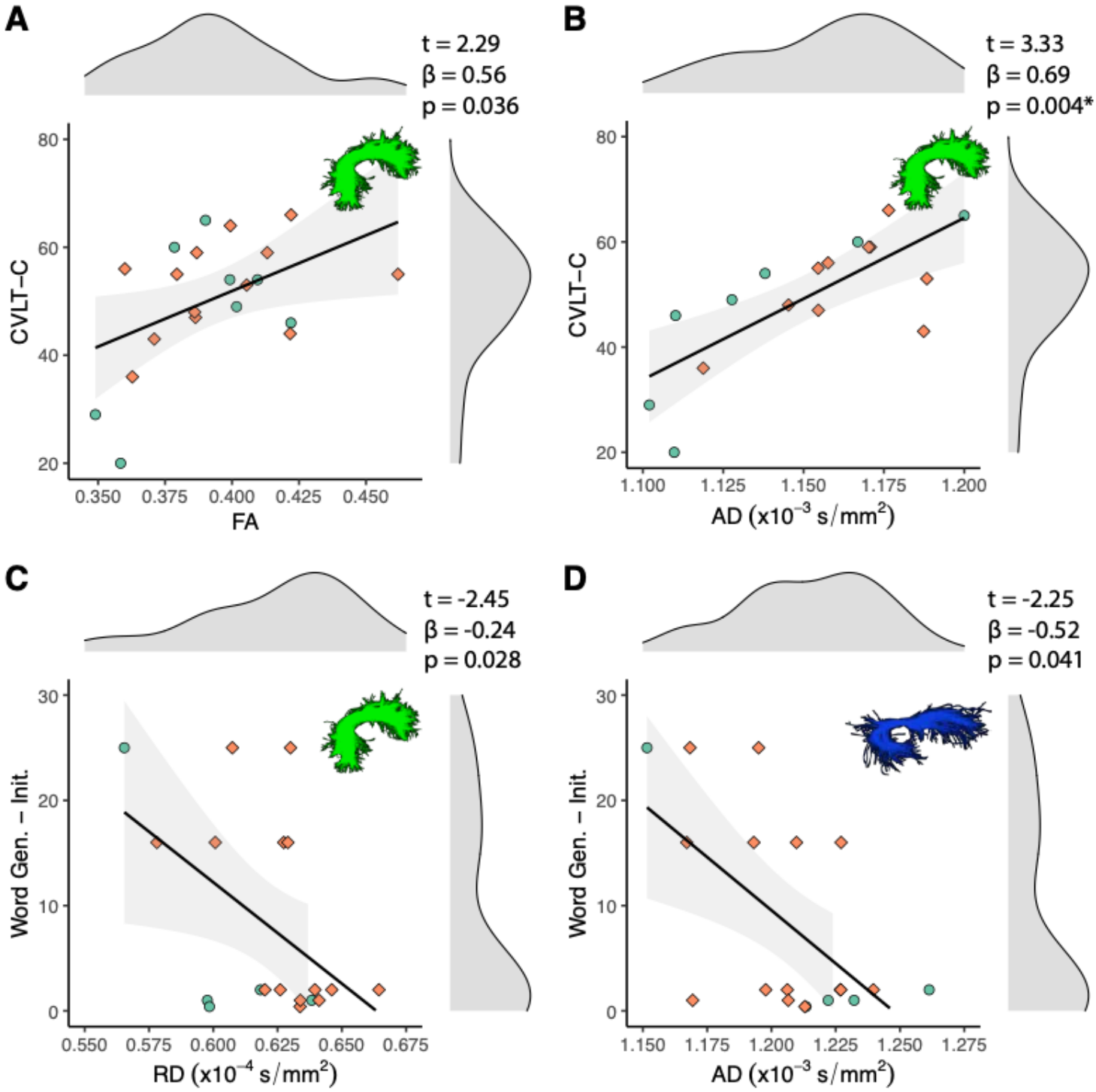


Figure 5

Associations between imaging metrics and language function in the contralesional arcuate (panels A, B, C) and uncinate (panel D) fasciculi in perinatal stroke participants, controlling for age, sex, and lesion volume. Fit lines with 95% confidence intervals are shown, along with plots visualizing data distribution. Data is split by sex, although no sex effects were observed (male: orange diamond, female: teal circle).